Remarkably Stable, High-Quality Semiconducting Single-Walled Carbon Nanotube Inks for Highly Reproducible Field-Effect Transistors

Talsma, Wytse; Sengrian, Aprizal Akbar; Salazar-Rios, Jorge Mario; Duim, Herman; Abdu-Aguye, Mustapha; Jung, Stefan; Allard, Sybille; Scherf, Ullrich; Loi, Maria Antonietta

Published in:
Advanced electronic materials

DOI:
10.1002/aelm.201900288

ADVANCED ELECTRONIC MATERIALS
www.advelectronicmat.de

Remarkably Stable, High-Quality Semiconducting Single-Walled Carbon Nanotube Inks for Highly Reproducible Field-Effect Transistors

*Wytse Talsma, Aprizal Akbar Sengrian, Jorge Mario Salazar-Rios, Herman Duim, Mustapha Abdu-Aguye, Stefan Jung, Sybille Allard, Ullrich Scherf, and Maria Antonietta Loi**

In the past years, high-quality semiconducting single-walled carbon nanotube (s-SWCNT) inks obtained by conjugated polymer wrapping using toluene as solvent have been used for the fabrication of high-performance field-effect transistors. Charge-carrier mobilities up to 50 $cm^2 V^{-1} s^{-1}$ and on/off ratios above 10^8 have been reported for devices based on networks of s-SWCNT. However, devices fabricated from inks that are only a few weeks old generally show a marked decrease in performance, indicating the limited shelf life of toluene-based inks. The use of o-xylene as applicator solvent to obtain high quality and very stable s-SWCNT inks is reported. The charge carrier mobility of field-effect transistors fabricated with this new ink show a twofold increase in magnitude compared to devices prepared from a toluene solution. More importantly, the device-to-device performance shows improved reproducibility, which is ascribed to the higher degree of homogeneity of the s-SWCNT network deposited from o-xylene with respect to the one from toluene. Finally, the o-xylene inks maintain their initial properties for longer than one year. This very long shelf life is an important pre-condition for the industrial use of s-SWCNT inks.

1. Introduction

In recent years, solution processable polymer-wrapped semiconducting single-walled carbon nanotubes (s-SWCNTs) have been intensively investigated due to their suitability for mass production of low-cost network field-effect transistors (FETs),[1] logic circuits,[2,3] and other electronic devices.[4–8] The polymer-wrapping selection of semiconducting SWCNT was introduced by Nish et al. in 2007,[9] and improved and expanded by many authors in the last years.[10–20] Polyfluorene,[18,21,22] polythiophene[23–26] derivatives, and many other polymers[27–32] are used to interact with the SWCNT walls.[33–36] However, the interaction of the polymer chains with the SWCNT is rather weak, resulting in the main advantage of this sorting method, namely the polymer wrapping does not greatly alter the electronic properties of the nanotubes.[37–39] In the last years, this technique has become very popular as compared with other solution-based selection processes such as density gradient ultracentrifugation and gel chromatography, in particular because of its simplicity, scalability, and high dispersion yield.[36,40,41]

The mechanism of the selection process of s-SWCNT, even if still under debate, can be described as following. First, the π–π interaction is driving the polymer backbone to the SWCNT walls, and the alkyl side chains wrap around the tube limiting its interaction with the solvent. Second, the selection mechanism, as it has been speculated, arises from the screening of the s-SWCNT polarizability by wrapped polymers.[12] The metallic-SWCNT (m-SWCNT) species have roughly three orders of magnitude larger polarizability as compared with the s-SWCNT.[42,43] It is, therefore, the large polarizability and the insufficient screening that lead to the rebundling of the m-SWCNT.[23] The significant weight difference between bundles and individualized tubes is the last ingredient, which allows for the separation of the two species by means of ultracentrifugation.

Not only the polymer structure but also the chain conformation in the solvent is an important factor to obtain high selectivity and high dispersion yield. Wang et al. investigated different organic solvents for the selection process bringing forward the idea that a poor solvent for the polymer is necessary to reduce the polymer–solvent interaction and favor the interaction with the SWCNT walls.[20] Toluene has been the most used solvent as it allows to obtain a good selection yield for semiconducting tubes with many different polymers.[11,13,18,24,44,45] Unfortunately, though, the shelf lifetime of s-SWCNT inks in toluene is severely limited by nanotube aggregation and

W. Talsma, A. A. Sengrian, Dr. J. M. Salazar-Rios,[+] H. Duim, M. Abdu-Aguye, Prof. M. A. Loi
Zernike Institute for Advanced Materials
University of Groningen
Nijenborgh 4, 9747 AG Groningen, The Netherlands
E-mail: m.a.loi@rug.nl
Dr. S. Jung, Dr. S. Allard, Prof. U. Scherf
Makromolekulare Chemie und Institut für Polymertechnologie
Bergische Universität Wuppertal
Gaußstraße 20, 42119 Wuppertal, Germany

The ORCID identification number(s) for the author(s) of this article can be found under https://doi.org/10.1002/aelm.201900288.

[+]Present address: Universidad de Manizales, Carrera 8 No 8–3, 170001 Manizales, Caldas, Colombia

DOI: 10.1002/aelm.201900288

twinning.[36] This is a big disadvantage for manufacturing of SWCNT-based devices on an industrial scale, using techniques such as inkjet-printing.[34,46,47]

In this work, we demonstrate the larger advantages of o-xylene over toluene as solvent for polymer-wrapped SWCNT. O-xylene is introduced as a solvent in the last step of the selection process, leaving the rest of the process unaffected. While the inks based on toluene strongly degrade after few months from their preparation, those in o-xylene maintain colloidal stability for longer than one year. This better colloidal stability has a big influence on the performance of fabricated devices. s-SWCNT field-effect transistors fabricated from o-xylene-based inks show an improvement in both charge carrier mobility and on/off ratio, and, most importantly, offer a much-enhanced device reproducibility.

We therefore demonstrate a massive enhancement of the ink shelf lifetime and of the overall FET performance by merely substituting the applicator solvent, indicating the suitability of these inks for mass production.

2. Results and Discussion

Figure 1a describes the procedure used for the semiconducting SWCNT selection and enrichment process using the polymer P3DDT.[35] The HiPCo SWCNT and the polymer are first sonicated together, allowing the s-SWCNT to be individualized and wrapped by the polymer. During the first centrifugation step, bundles of m-SWCNT together with other carbon contaminants precipitate due to their weight. Upon completion of the centrifugation step, the supernatant, which contains the desired s-SWCNT wrapped by the polymer as well as the excess of free polymer, is extracted. In order to remove the excess polymer, a second centrifugation step is performed, which we refer to as the enrichment. At this point, the precipitated pellet contains the polymer-wrapped s-SWCNT while the excess polymer is in the supernatant. The pellet is therefore removed and re-dispersed either in toluene or in o-xylene, which we refer to in the following as applicator solvents.

Toluene is the most common applicator solvent for polymer-wrapped SWCNT inks and has been used with success in the last 10 years of research in the field.[13,19,20,35,45,48–50] Here we aim to investigate the stability of inks based on toluene and to compare their performance with inks using o-xylene as applicator solvent.

Figure 1b shows the s-SWCNT inks in both solvents freshly prepared and after one year aging. For the one-year-old toluene-based ink, small aggregates are visible as suspensions in the solution; this results in an overall lower optical density. Instead, the one-year-old o-xylene solution has the same appearance as the freshly made ink.

The variation that occurred in the solutions is quantified by absorption spectroscopy. **Figure 2**a shows the absorption spectra of the s-SWCNT ink in toluene as prepared and after one year from its preparation, almost half of the optical absorption is lost in one year. The overall intensity of the absorption is reduced because of the formation of aggregates, as the bundled SWCNTs do not contribute significantly (vide infra) to the S_{11} transition. The aggregate formation could be attributed to the poor solubility of the polymer-wrapped s-SWCNT in toluene

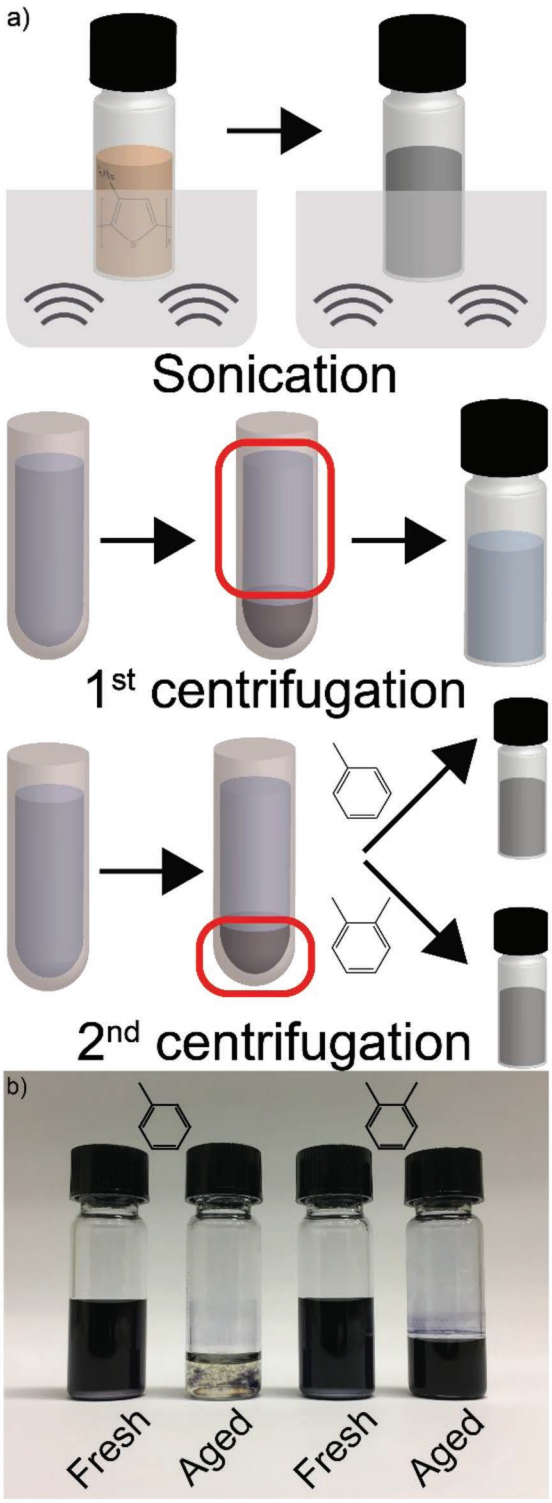

Figure 1. a) Schematic illustration showing the different steps in the selection process as initially described by Bisri et al.[53] First, the polymer is solubilized by stirring and sonication in toluene, then the pristine carbon nanotubes are added. After sonication, the mixture goes through two different centrifugation steps. Finally, the pellet is redispersed. In this study, pellets are redispersed into either toluene or o-xylene. b) The toluene- and o-xylene-based s-SWCNT inks when freshly prepared, and after aging for a period of one year. Agglomeration is clearly visible for the ink in toluene.

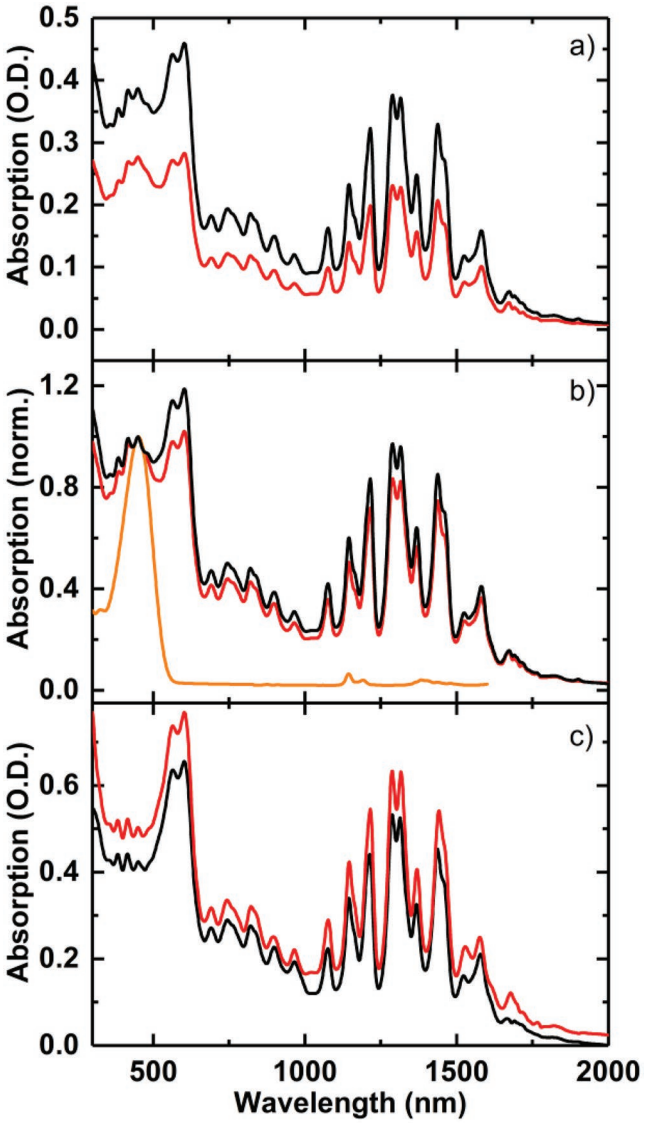

Figure 2. Absorption spectra of a) toluene-based s-SWCNT inks fresh and one year old, black and red curves, respectively. b) Absorption spectra of s-SWCNT inks in toluene as in (a), in orange the spectra of the pristine P3DDT polymer solution. All spectra are normalized to the 450 nm peak. c) Absorption spectra of the s-SWCNT inks in o-xylene fresh and one-year-old, black and red curves, respectively.

and to the tendency of the P3DDT polymer side chains to intertwine between themselves.[20] We have reported earlier that the intertwining of the P3DDT side chains is responsible for the formation of s-SWNT twins in P3DDT-wrapped s-SWCNT.[36]

Besides the overal difference in intensity, the two absorption spectra in Figure 2a show another important difference. To highlight the difference in Figure 2b, the absorption spectra are reproduced normalized with respect to the peak at 450 nm. This peak is determined by the free polymer chain absorption (see also the reference spectra in orange in Figure 2b) and shows a blueshift with respect to the two features at 564 and 604 nm, which are typical of the P3DDT aggregation around the carbon nanotube walls.[36] The relative increase of free polymer absorption in the one-year-old solution indicates unwrapping of a portion of the s-SWCNT, which in turn explains the loss of individualization. Therefore we can conclude that in the case of the toluene solution two main effects determine the limited shelf lifetime, namely, the unwrapping of the polymer and the formation of aggregates driven by the polymer alkyl chains.

As observed above, there is no variation in the appearance of the SWCNT dispersion in o-xylene even after storage for one year. By measuring the absorption spectra of the two s-SWCNT inks in o-xylene (Figure 2c), we evidence an increase of the overall sample absorption intensity in the aged sample, verisimilarly determined by the increase in concentration due to the slow solvent evaporation from the ink in the storage unit. We can therefore state that the s-SWCNT ink in o-xylene features a shelf life of at least one year, which is the time we have been monitoring its stability, which does not exclude a much longer shelf life.

To further investigate the quality and stability of the inks, steady-state and time-resolved photoluminescence (PL) spectroscopy are used. In **Figure 3**a, the steady-state PL spectra of the two freshly prepared samples are reported. The PL intensity of the four highest energy bandgap SWCNTs is substantially higher (50%), in the o-xylene-based samples with respect to the toluene one, at parity of concentration. As aggregation of SWCNT is generally responsible for energy transfer and nonradiative recombination, the increase of the PL intensity indicates a better individualization of the s-SWCNT in the o-xylene-based sample. It is interesting to note that the two lower bandgap tubes, namely, at 1373 and 1440 nm, show instead identical PL intensity for the two samples. In other words, the relative intensity between the higher energy peaks and the lower energy ones is smaller for the toluene-based solutions. This is an indication of the fact that energy transfer is occurring between larger bandgap SWCNT and smaller bandgap one in the case of toluene-based solutions, while in the case of o-xylene-based one this transfer is either less efficient or totally suppressed. In agreement with this observation, there is an improvement of the lifetime for both the short (t_1) and long (t_2) components of the PL decay of the SWCNT S_{11} transition at 1080 nm, as reported in Figure 3b. The components t_1 and t_2 are 3 and 19 ps for the toluene-based sample and, 12 and 44 ps for the o-xylene one. This is a further strong evidence of the better individualization of the s-SWCNT o-xylene with respect to toluene.

The ultimate proof of the quality of the inks is obtained by using them for the fabrication of FETs. To this purpose, FETs were fabricated from both toluene-based and o-xylene-based inks that were freshly prepared or had been in storage for one year. It is important to note that inks were not sonicated prior to deposition. In fact, s-SWCNT aggregations can be partially removed by mild sonication. In **Figure 4**a are reported the typical output characteristics obtained from FETs fabricated with freshly prepared P3DDT-wrapped s-SWCNT inks in o-xylene (top) and toluene (bottom) with identical initial concentrations as determined from absorption. The devices show a pronounced p-type behavior with the sample deposited from o-xylene showing a factor two higher current with respect to the one from toluene. In this type of s-SWCNT network based transistors the current magnitude depends on the number of

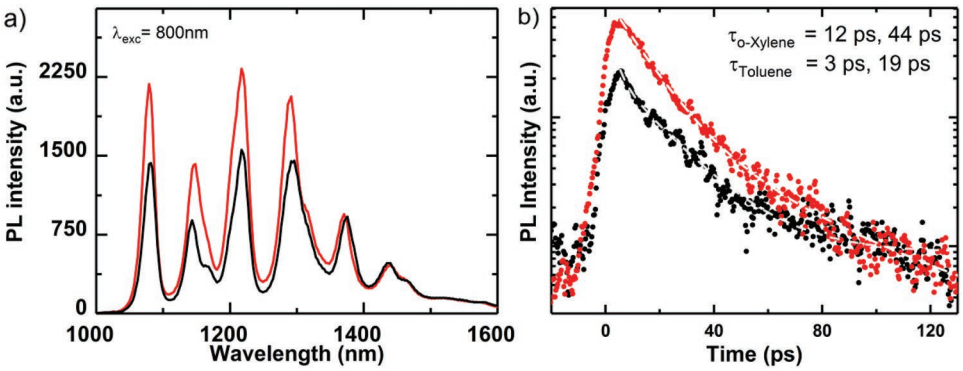

Figure 3. a) Steady-state photoluminescence of the s-SWCNT inks in o-xylene (red) and toluene (black); b) time-resolved photoluminescence of the s-SWCNT peak at 1080 nm. The white dashed lines are the bi-exponential fit.

tubes crossing the transistor channel, we argue that in the case of aged o-xylene-based inks a better distribution of s-SWCNT is obtained, forming a more extended percolation network. In **Figure 5** are shown the typical transfer characteristics obtained from FETs fabricated with the two inks, the red curve for the o-xylene- and the black curve for the toluene-based one. The fresh solutions show very similar performances for the hole current and a small difference in the electron current. The toluene solution shows a higher off-current.

Devices fabricated from one-year-old solutions show the largest difference in performances. The toluene-based inks show a significant deterioration in performance for both hole- and electron-transport, as compared with devices fabricated from fresh inks, see output characteristics in Figure 4b. The hole I_{on} shows a reduction of one-and-a-half order of magnitude (see Figure 5). This also affects the hole mobility, which is reduced from 1.8 to 4.4 × 10^{-2} cm^2 V^{-1} s^{-1}. Additionally, the electron mobility decreases from 0.4 to 3.5 × 10^{-3} cm^2 V^{-1} s^{-1}. Moreover, the higher subthreshold swing (SS) (especially in the electron-side) indicates an increase in trap density, leading to noncomparable extracted threshold voltages V_{th}.[51] This increase of the SS may be explained by a higher interaction of the s-SWCNT network with the SiO_2 surface due to the previously discussed unwrapping of the polymer chains.

In contrast, devices prepared using one-year-old o-xylene-based inks show a similar I_{on} for both fresh and aged solutions (Figures 4b and 5). Moreover, mobilities obtained from these devices show surprisingly, that while the electron mobility decreases from 0.5 to 0.4 cm^2 V^{-1} s^{-1}, the hole mobility increases from 1.7 to 1.9 cm^2 V^{-1} s^{-1} going from the fresh to the one-year-old solution.

A summary of the FET performance distribution of devices fabricated with freshly prepared o-xylene and toluene inks is reported in **Figure 6**. It is evident from Figure 6a,b that the

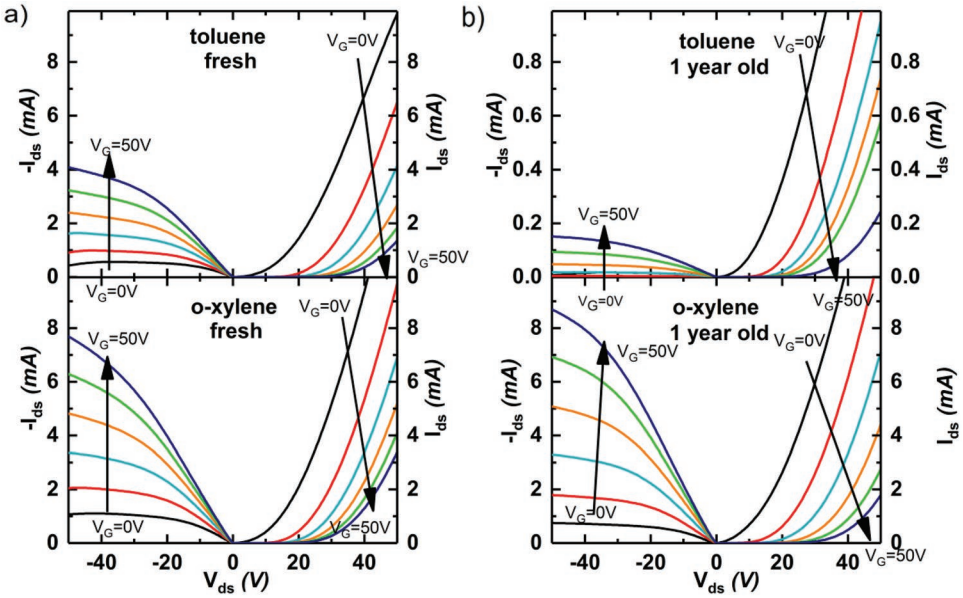

Figure 4. a) Output characteristics of FETs fabricated using toluene and o-xylene s-SWCNT inks of freshly prepared solutions. b) Characteristics of devices fabricated with one-year aged toluene and o-xylene solutions.

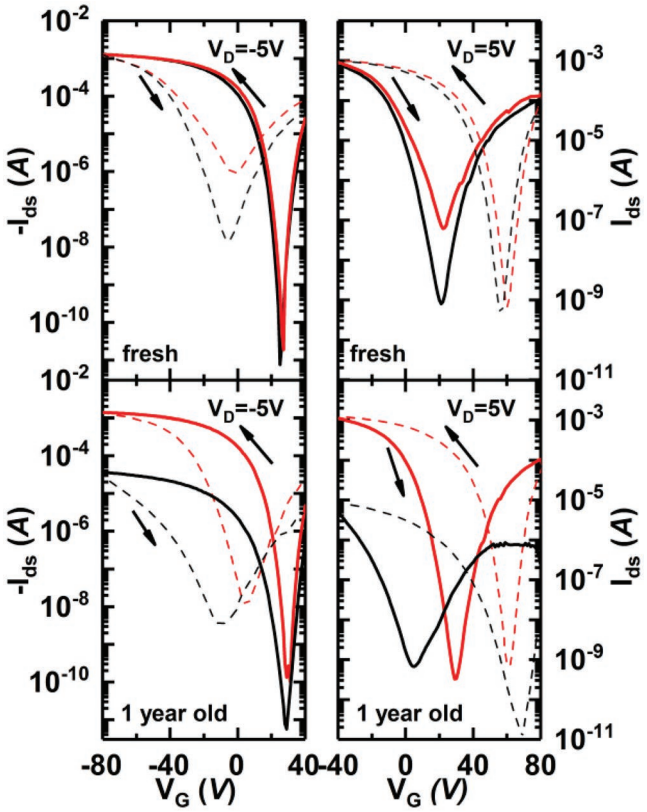

Figure 5. Transfer characteristics at V_D = 5 V of FETs fabricated using toluene (black) and o-xylene (red) s-SWCNT inks; top panels: devices fabricated from freshly prepared solutions, bottom panels: devices fabricated from one-year-old solutions. The reverse curves are displayed as dashed lines.

variation in device characteristics for o-xylene-based inks is significantly lower than for toluene-based inks. The o-xylene inks show an average higher mobility (117% higher hole mobility than for toluene inks) and a peak on–off ratio of 10^{10}, even if on average the on–off ratio does not show significant differences.

At this point, it is important to understand why FET devices deposited from o-xylene-based solutions are on average better performing than the ones based on toluene.

A direct effect of the improved individualization is a higher number of SWCNT-SWCNT junctions, which will increase the density of tubes on the surface and consequently improves the percolation pathway. The AFM microscopy images reported in Figure S1 (Supporting Information) seem to support this idea. In fact, the comparison between Figure S1a,b (Supporting Information), which shows the SWCNT network deposited on a SiO_2 surface from the toluene- and o-xylene-based inks, respectively, shows a lower degree of large bundles and crossing points for the last. From Figure S1c,d (Supporting Information) it is evident that the tendency to aggregate increases with time and that the network deposited from 12-months-old toluene ink results in large aggregates of SWCNT, while the SWCNT in o-xylene maintains a large degree of individualization even after a long time in solution.

Apart from the improved individualization of s-SWCNT, also the better wetting of the SiO_2 surface obtained with the o-xylene-based inks can be the reason of a higher homogeneity and densities of the networks obtained. This could, in turn, explain the device reproducibility. This hypothesis is supported by contact angle measurements (Figure S2, Supporting Information), showing a lower contact angle (9.5°) for o-xylene-based inks compared to the toluene one (12.4°). Alternatively, the difference in contact angle being so small, one could argue that the difference in boiling point and evaporation kinetics between the two solvents can also contribute to determine the difference between our s-SWCNT networks.

The main quality of the o-xylene-based inks is, therefore, the higher device reproducibility and the extremely long shelf lifetime. This has an enormous importance for commercial applications. Not only when considering large surface deposition

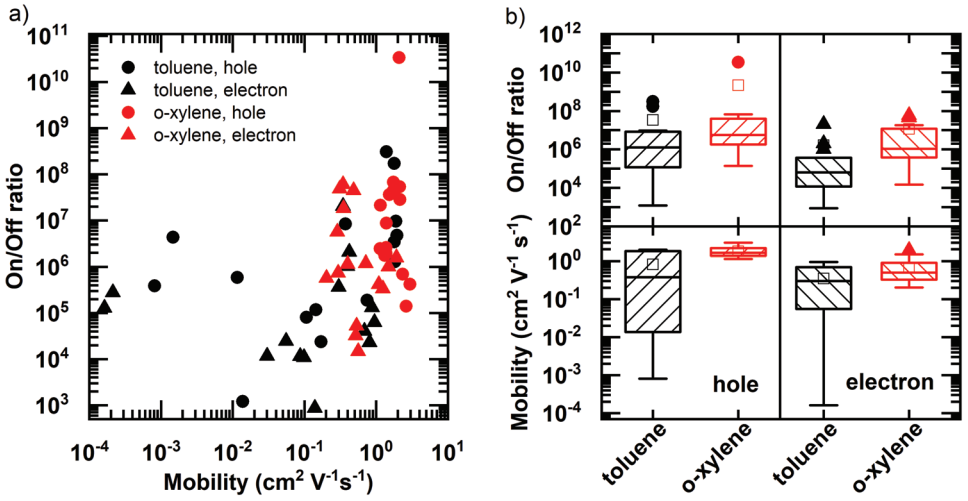

Figure 6. s-SWCNT FET performance distribution. a) Hole (circle) and electron (triangle) mobilities versus on/off ratio of devices fabricated with s-SWCNT inks in toluene (black) and o-xylene (red). b) Statistical representation of the same data as in (a), with on the left side the distribution for holes and the right side for electrons.

techniques as blade coating but also for techniques as inkjet printing where solvents with a high boiling point as well as lower toxicity are required.

3. Conclusion

We demonstrated that merely substituting the applicator solvent in a colloidal dispersion of polymer-wrapped semiconducting-SWCNT results in an improvement in both shelf lifetime (longer than one year) and FET performance and reproducibility.

By substituting toluene with o-xylene, the chirality distribution in the dispersion remains unaffected. Moreover, a similar distribution of SWCNT is obtained when depositing the two inks. However, the better wetting allows for a more homogeneous distribution of SWCNT cast from o-xylene, which improves the percolation network for charge carriers. Consequently, the average FET mobilities are improved over two folds for inks using o-xylene and the overall reproducibility is enhanced.

These results represent an important step toward the large-scale technological utilization of s-SWCNT inks for electronic and optoelectronic applications.

4. Experimental Section

Polymer Synthesis: The homopolymer P3DDT was synthesized via the GRIM method and the molecular weight was measured using gel permeation chromatography (GPC).[52] The polymer was obtained after the Soxhlet extraction with methanol, acetone, ethyl acetate, and hexane. For the herein reported experiments the narrowly distributed hexane fraction with M_n/M_w 19 200/22 300 g mol^{-1} (polydispersity index PDI: 1.16) was used.

Preparation and Characterization of s-SWCNT Dispersion: HiPCo SWCNT (0.8–1.2 nm) were purchased from Unidym Inc. First the polymer was solubilized in toluene, subsequently SWCNT was added to form the SWCNT:polymer dispersion at a weight ratio of 1:2 (3 mg of SWCNT, 6 mg of polymer, 15 mL of toluene), the solution was then sonicated in a cup-horn for 2 h at 78 W. After ultrasonication, the dispersion was centrifuged at 30 000 rpm (109 000 g) for 1 h in an ultracentrifuge (Beckman Coulter Optima XE-90; rotor: SW55Ti). After the centrifugation, the highest density components precipitated at the bottom of the centrifugation tube, while the low-density components, including small bundles and individualized SWCNTs wrapped by the polymer, and free polymer chains, remained in the upper part as supernatant. One extra step of ultracentrifugation was implemented to decrease the amount of excess polymer in solution (enrichment).[53] In this step the supernatant obtained after the first ultracentrifugation was centrifuged for 5 h at 55 000 rpm (367 000 g). At this point, the individualized s-SWCNTs precipitated to form a pellet, and the free polymer remained in the supernatant. Finally, the pellet was taken away and re-dispersed by sonication in o-xylene or in toluene.

Optical Characterization of the s-SWNT Dispersion: Optical measurements were performed to check the concentration of semiconducting carbon nanotubes selected by the polymer and to monitor the colloidal stability of the ink over time. Absorption spectra were recorded with a UV–vis–NIR spectrophotometer (Shimadzu UV-3600).

For the PL measurements the samples were excited at ≈800 nm by the fundamental mode of a mode-locked Ti:Sapphire laser (Mira 900, Coherent). A variable neutral density filter was used to adjust the laser excitation power on the sample. The PL decays were recorded with an NIR sensitive Hamamatsu streak camera working in synchroscan mode (time resolution ≈2 ps). The steady-state PL spectra were measured with an InGaAs Andor inline detector, and corrected for the spectral response of the setup using a calibrated light source.

Fitting and Data Analysis for Optical Measurements: Steady-state spectra were fitted with Gaussian functions (the average goodness-of-fit was determined by the chi-squared (χ^2) test). Lifetimes were fitted using exponential functions such as $I = \sum_i A_i \exp(-t/\tau_i)$. When only one lifetime was reported, the best fit could be achieved with a monoexponential function; otherwise a bi-exponential function was used.

FET Transistor Fabrication and Electrical Characterization: Field-effect transistors were fabricated on silicon substrates with on top a thermally grown SiO_2 dielectric layer (230 nm thickness). Source and drain bottom electrodes (10 nm ITO/30 nm Au) were lithographically patterned forming an interdigitated channel. The different s-SWCNT dispersions tested were deposited in a nitrogen-filled glove box by blade coating (Zehntner ZAA 2300 Automatic film applicator coater). The deposition procedure was repeated two times to achieve a sufficiently high s-SWCNT coverage density. After deposition, the samples were annealed at 160 °C for 60 min to evaporate the remaining solvent.

Electrical measurements were performed using a probe station placed in a nitrogen-filled glove box at room temperature under dark conditions. The probe station is connected to an Agilent E5262A Semiconductor Parameter Analyzer. The reported charge carrier mobilities were extracted from the I_{DS}–V_G transfer characteristics in the linear regime at $V_D = \pm 5$ V. The gate capacitance was corrected from the parallel plate capacitance taking into account the linear density of the s-SWCNT network and quantum capacitance of the s-SWCNT as described by Cao et al.[54]

Supporting Information

Supporting Information is available from the Wiley Online Library or from the author.

Acknowledgements

The authors are thankful to A. Kamp and T. Zaharia for technical support. The authors are thankful to C. Richards for the help with the contact angle measurements. This work is partly financed by the Dutch Research Council (NWO).

Conflict of Interest

The authors declare no conflict of interest.

Keywords

field-effect transistors, polymer wrapping, single-walled carbon nanotubes

Received: March 19, 2019
Revised: May 21, 2019
Published online: June 27, 2019

[1] S. J. Tans, A. R. M. Verschueren, C. Dekker, *Nature* **1998**, *393*, 49.
[2] M. M. Shulaker, G. Hills, N. Patil, H. Wei, H.-Y. Chen, H.-S. P. Wong, S. Mitra, *Nature* **2013**, *501*, 526.
[3] K. Kim, C. L. Chen, Q. Truong, A. M. Shen, Y. Chen, *Adv. Mater.* **2013**, *25*, 1693.

[4] E. S. Snow, F. K. Perkins, J. A. Robinson, *Chem. Soc. Rev.* **2006**, *35*, 790.
[5] J. P. Novak, E. S. Snow, E. J. Houser, D. Park, J. L. Stepnowski, R. A. McGill, *Appl. Phys. Lett.* **2003**, *83*, 4026.
[6] A. T. Charlie Johnson, C. Staii, M. Chen, S. Khamis, R. Johnson, M. L. Klein, A. Gelperin, *Physica Status Solidi B* **2006**, *243*, 3252.
[7] M. Jung, J. Kim, J. Noh, N. Lim, C. Lim, G. Lee, J. Kim, H. Kang, K. Jung, A. D. Leonard, J. M. Tour, G. Cho, *IEEE Trans. Electron Devices* **2010**, *57*, 571.
[8] F. Wang, Y. Yang, T. M. Swager, *Angew. Chem., Int. Ed.* **2008**, *47*, 8394.
[9] A. Nish, J.-Y. Hwang, J. Doig, R. J. Nicholas, *Nat. Nanotechnol.* **2007**, *2*, 640.
[10] S. K. Samanta, M. Fritsch, U. Scherf, W. Gomulya, S. Z. Bisri, M. A. Loi, *Acc. Chem. Res.* **2014**, *47*, 2446.
[11] W. Gomulya, G. D. Costanzo, E. J. F. De Carvalho, S. Z. Bisri, V. Derenskyi, M. Fritsch, N. Fröhlich, S. Allard, P. Gordiichuk, A. Herrmann, S. J. Marrink, M. C. Dos Santos, U. Scherf, M. A. Loi, *Adv. Mater.* **2013**, *25*, 2948.
[12] W. Gomulya, V. Derenskyi, E. Kozma, M. Pasini, M. A. Loi, *Adv. Funct. Mater.* **2015**, *25*, 5858.
[13] A. Graf, Y. Zakharko, S. P. Schießl, C. Backes, M. Pfohl, B. S. Flavel, J. Zaumseil, *Carbon* **2016**, *105*, 593.
[14] S. P. Schießl, N. Fröhlich, M. Held, F. Gannott, M. Schweiger, M. Forster, U. Scherf, J. Zaumseil, *ACS Appl. Mater. Interfaces* **2015**, *7*, 682.
[15] F. Bottacchi, L. Petti, F. Späth, I. Namal, G. Tröster, T. Hertel, T. D. Anthopoulos, *Appl. Phys. Lett.* **2015**, *106*, 193302.
[16] T. Lei, I. Pochorovski, Z. Bao, *Acc. Chem. Res.* **2017**, *50*, 1096.
[17] P. Gerstel, S. Klumpp, F. Hennrich, A. Poschlad, V. Meded, E. Blasco, W. Wenzel, M. M. Kappes, C. Barner-Kowollik, *ACS Macro Lett.* **2014**, *3*, 10.
[18] J. Gao, M. A. Loi, E. J. F. De Carvalho, M. C. Dos Santos, *ACS Nano* **2011**, *5*, 3993.
[19] K. S. Mistry, B. A. Larsen, J. L. Blackburn, *ACS Nano* **2013**, *7*, 2231.
[20] H. Wang, B. Hsieh, G. Jiménez-Osés, P. Liu, C. J. Tassone, Y. Diao, T. Lei, K. N. Houk, Z. Bao, *Small* **2015**, *11*, 126.
[21] M. C. Gwinner, F. Jakubka, F. Gannott, H. Sirringhaus, J. Zaumseil, *ACS Nano* **2012**, *6*, 539.
[22] A. Chortos, I. Pochorovski, P. Lin, G. Pitner, X. Yan, T. Z. Gao, J. W. F. To, T. Lei, J. W. Will, H. S. P. Wong, Z. Bao, *ACS Nano* **2017**, *11*, 5660.
[23] J. M. Salazar-Rios, W. Talsma, V. Derenskyi, W. Gomulya, T. Keller, M. Fritsch, S. Kowalski, E. Preis, M. Wang, S. Allard, G. C. Bazan, U. Scherf, M. C. dos Santos, M. A. Loi, *Small Methods* **2018**, *2*, 1700335.
[24] H. Wang, G. I. Koleilat, P. Liu, G. Jiménez-Osés, Y. C. Lai, M. Vosgueritchian, Y. Fang, S. Park, K. N. Houk, Z. Bao, *ACS Nano* **2014**, *8*, 2609.
[25] H. W. Lee, Y. Yoon, S. Park, J. H. Oh, S. Hong, L. S. Liyanage, H. Wang, S. Morishita, N. Patil, Y. J. Park, J. J. Park, A. Spakowitz, G. Galli, F. Gygi, P. H. S. Wong, J. B. H. Tok, J. M. Kim, Z. Bao, *Nat. Commun.* **2011**, *2*, 541.
[26] D. Ji, S. H. Lee, Y. Y. Noh, *Appl. Phys. Lett.* **2018**, *112*, 2.
[27] T. Fujigaya, N. Nakashima, *Sci. Technol. Adv. Mater.* **2015**, *16*, 024802.
[28] M. Shigeta, M. Komatsu, N. Nakashima, *Chem. Phys. Lett.* **2006**, *418*, 115.
[29] T. Fukumaru, T. Fujigaya, N. Nakashima, *Macromolecules* **2013**, *46*, 4034.
[30] J. Yoo, T. Fujigaya, N. Nakashima, *Nanoscale* **2013**, *5*, 7419.
[31] J. Yoo, H. Ozawa, T. Fujigaya, N. Nakashima, *Nanoscale* **2011**, *3*, 2517.
[32] A. B. Dalton, C. Stephan, J. N. Coleman, B. McCarthy, P. M. Ajayan, S. Lefrant, P. Bernier, W. J. Blau, H. J. Byrne, *J. Phys. Chem. B* **2000**, *104*, 10012.
[33] V. Derenskyi, W. Gomulya, J. Gao, S. Z. Bisri, M. Pasini, Y. L. Loo, M. A. Loi, *Appl. Phys. Lett.* **2018**, *112*, 072106.
[34] J. Zaumseil, *Semicond. Sci. Technol.* **2015**, *30*, 074001.
[35] V. Derenskyi, W. Gomulya, J. M. S. Rios, M. Fritsch, N. Fröhlich, S. Jung, S. Allard, S. Z. Bisri, P. Gordiichuk, A. Herrmann, U. Scherf, M. A. Loi, *Adv. Mater.* **2014**, *26*, 5969.
[36] W. Gomulya, J. M. S. Rios, V. Derenskyi, S. Z. Bisri, S. Jung, M. Fritsch, S. Allard, U. Scherf, M. C. Dos Santos, M. A. Loi, *Carbon* **2015**, *84*, 66.
[37] M. S. Strano, C. A. Dyke, M. L. Usrey, P. W. Barone, M. J. Allen, H. Shan, C. Kittrell, R. H. Hauge, J. M. Tour, R. E. Smalley, *Science* **2003**, *301*, 1519.
[38] M. Kanungo, H. Lu, G. G. Malliaras, G. B. Blanchet, *Science* **2009**, *323*, 234.
[39] S. Kahmann, J. M. Salazar Rios, M. Zink, S. Allard, U. Scherf, M. C. Dos Santos, C. J. Brabec, M. A. Loi, *J. Phys. Chem. Lett.* **2017**, *8*, 5666.
[40] H. W. Lee, Y. Yoon, S. Park, J. H. Oh, S. Hong, L. S. Liyanage, H. Wang, S. Morishita, N. Patil, Y. J. Park, J. J. Park, A. Spakowitz, G. Galli, F. Gygi, P. H.-S. Wong, J. B.-H. Tok, J. M. Kim, Z. Bao, *Nat. Commun.* **2011**, *2*, 541.
[41] C. Wang, K. Takei, T. Takahashi, A. Javey, *Chem. Soc. Rev.* **2013**, *42*, 2592.
[42] E. Joselevich, C. M. Lieber, *Nano Lett.* **2002**, *2*, 1137.
[43] Z. Wang, C. Tang, R. Sachs, Y. Barlas, J. Shi, *Phys. Rev. Lett.* **2015**, *114*, 016603.
[44] F. Jakubka, C. Backes, F. Gannott, U. Mundloch, F. Hauke, A. Hirsch, J. Zaumseil, *ACS Nano* **2013**, *7*, 7428.
[45] J.-Y. Hwang, A. Nish, J. Doig, S. Douven, C.-W. Chen, L.-C. Chen, R. J. Nicholas, *J. Am. Chem. Soc.* **2008**, *130*, 3543.
[46] S. G. Bucella, J. M. Salazar-Rios, V. Derenskyi, M. Fritsch, U. Scherf, M. A. Loi, M. Caironi, *Adv. Electron. Mater.* **2016**, *2*, 1600094.
[47] Z. Liu, J. Zhao, W. Xu, L. Qian, S. Nie, Z. Cui, *ACS Appl. Mater. Interfaces* **2014**, *6*, 9997.
[48] H. Zhang, L. Xiang, Y. Yang, M. Xiao, J. Han, L. Ding, Z. Zhang, Y. Hu, L. M. Peng, *ACS Nano* **2018**, *12*, 2773.
[49] J. Gu, J. Han, D. Liu, X. Yu, L. Kang, S. Qiu, H. Jin, H. Li, Q. Li, J. Zhang, *Small* **2016**, *12*, 4993.
[50] V. Derenskyi, W. Gomulya, W. Talsma, J. M. Salazar-Rios, M. Fritsch, P. Nirmalraj, H. Riel, S. Allard, U. Scherf, M. A. Loi, *Adv. Mater.* **2017**, *29*, 1606757.
[51] G. Horowitz, R. Hajlaoui, H. Bouchriha, R. Bourguiga, M. Hajlaoui, *Adv. Mater.* **1998**, *10*, 923.
[52] R. S. Loewe, S. M. Khersonsky, R. D. McCullough, *Adv. Mater.* **1999**, *11*, 250.
[53] S. Z. Bisri, J. Gao, V. Derenskyi, W. Gomulya, I. Iezhokin, P. Gordiichuk, A. Herrmann, M. A. Loi, *Adv. Mater.* **2012**, *24*, 6147.
[54] Q. Cao, M. Xia, C. Kocabas, M. Shim, J. A. Rogers, S. V. Rotkin, *Appl. Phys. Lett.* **2007**, *90*, 2005.